

## Water Characterization and Seasonal Heavy Metal Distribution in the Odiel River (Huelva, Spain) by Means of Principal Component Analysis

C. Montes-Botella,<sup>1</sup> M. D. Tenorio<sup>2</sup>

<sup>1</sup> Department of Statistics and Econometrics, Universidad Carlos III de Madrid, c/ Butarque, 15, 28911-Leganés, Madrid, Spain

<sup>2</sup> Department of Bromatology II, Universidad Complutense de Madrid, Ciudad Universitaria, s/n. 28040-Madrid, Madrid, Spain

Received: 9 July 2002/Accepted: 22 April 2003

**Abstract.** The Iberian Pyrite Belt is the largest mass of sulfide and manganese ores in Western Europe. Its sulfide oxidation is the origin of a heavily acidic drainage that affects the Odiel River in southwestern Huelva (Spain). To assess physicochemical, contamination parameters, heavy metal distribution and its seasonal variation in the upper Odiel River and in El Lomero mines, three water samplings were undertaken and analyzed between July 1998 and November 1999. Water from the Odiel River in the polluted zone showed low pH values (2.76–3.51), high heavy metal content, and high values of conductivity (1410–3648  $\mu\text{S}/\text{cm}$ ) and dissolved solids (1484–5602 mg/L). Principal Component Analysis (PCA) showed that variables related with the products of the pyrite oxidation and the salts that are solubilized by the high acidity generated in the oxidation of sulfides, grouped in the first component, accounted for 40.88% of total variance, and were the main influential factor in physicochemical water sample properties. The second influential factor was minority metals (nickel, cobalt, cadmium). Heavy metals showed three different seasonal patterns, closely related with saline efflorescences formed next to the river bed: majority metals (iron, copper, manganese, zinc); minority metals (lead, nickel, cobalt, cadmium); and chromium, which had a distinctive behavior.

the Huelva Province (IGME 1982). These deposits typically contain 50% sulfur, 42% iron, 2–8% copper, lead, and zinc by weight and significant quantities of gold and silver (van Geen *et al.* 1999).

The Odiel River has its source in the Sierra de Aracena y Picos de Aroche natural park. It is a relatively small river (128 km in length, 3 m<sup>3</sup>/s mean water discharge) and it delimits the boundaries of the Riotinto mining area. The oxidation of pyrite in the mining zone gives rise to large quantities of H<sup>+</sup> (Lowson 1982), and as a consequence, Odiel water is strongly acidic. The mine waters affected by pyrite oxidation process may show great variability in their physicochemical characteristics, but they usually have elevated concentrations of sulfate, iron, and heavy metals (Caruccio *et al.* 1989; Evangelou and Zhang 1995). Acidic mine drainage, caused by sulfide oxidation, is a major water quality problem throughout the world (Gray 1997). The Tinto-Odiel fluvial system has therefore been extensively studied because of its discharges in Gulf of Cadiz (García Vargas *et al.* 1980; Nelson and Lamothe 1993; van Geen *et al.* 1997; Elbaz-Poulichet *et al.* 1999). In this paper, we study the upstream zone (Figure 1), where acid discharges occur, to assess heavy metal behavior in these extremely high acid and salt conditions.

El Andévalo is a region located in the middle zone between the coastal plains and Aracena Mountains in the north of Huelva, Spain. It includes the mining area of Riotinto, between the Tinto and Odiel Rivers. It is part of the Iberian Pyrite Belt, the largest mass of sulfides and manganese ores in Western Europe, which has been exploited since 2500 year BC (Belén 2000). It spans 200 km, from the Caveira Mountains (Southwest Portugal) to Aznalcóllar (Sevilla), where it is covered by tertiary materials at the Guadalquivir Depression (Rambaud Pérez 1963; Quesada 1996). The most important mineral ore mines (Riotinto, Tharsis, and Sotiel-Coronada) are located in

### Material and Methods

We consider five sampling zones in our study—four in the Odiel River, with one control point (OD-A, see below), and one in a nearby contaminated area (Figure 1)—as follows: (1) OD-A, upper Odiel, between Aracena and Campofrío districts. No contamination. Pasture meadows. UTM coordinates, 29S QB156-867. (2) OD-B, middle Odiel, between El Campillo and Almonáster districts. Polluted area; yellowish water, without macroscopic biological activity. The only species growing close to the river is *Erica andevalensis* Cabezudo and Rivera, a plant endemism exclusive to this area. UTM coordinates, 29S QB022-781. (3) OD-C, Odiel river, between Calañas and Zalamea la Real districts. Polluted area; yellowish water, without macroscopic biological activity. River bed. UTM coordinates, 29S PB927-694. (4) OD-D, Odiel river, between Calañas and Valverde del Camino districts, near Sotiel-Coronada. Contaminated area. Working mine. UTM coordinates, 29S PB916-644. (5) LOM, ascent to El Lomero mines, located in El Cerro de Andévalo district. Pools with lixiviated water



Fig. 1. Map of the Upper Odiel River (Huelva, Spain) with sampling zones

from the mine (occasionally dried) and heavily yellow water course, without visible biological activity. UTM coordinates, 29S PB933-862.

Three sampling expeditions were carried out between July 1998 and November 1999. Simple samples were taken from the stream center and surface, transported to the laboratory, measured for turbidity by nephelometric method with photometer Merck SQ 300, filtered, and stored at 2°C until completion of the analysis. All chemicals used were of reagent grade and were purchased from Merck (Merck K GaA, Darmstadt).

### Experimental Methods

Temperature was the only measure taken "in situ" (APHA 1998; Rodier 1998). pH was measured with a pH meter (Crison micro pH 2000), after calibration with standard pH buffers (APHA 1998). Conductivity was measured with conductimeter (Radiometer Type CDM), after calibration with conductivity standard solutions (APHA 1998); residue dried (or total dissolved solids at 180°C, TDS) by evaporating water sample and subsequently desiccating it (180°C) to constant weight (APHA 1998). Hardness was measured by EDTA titrimetric method (Rodier 1998); chloride was measured by argentometric (Mohr) procedure (APHA 1998); bicarbonates by volumetric method, with HCl 0.01 N (Rodier 1998); silica by silicomolybdate photometric method (Blasco Gordo 1983); sulfate

by gravimetric method; calcium and magnesium by complexometric method; sodium and potassium by air-acetylene flame photometry (APHA 1998), after redissolution of the residue dried with HCl-HNO<sub>3</sub> 50% and cesium chloride addition, with an atomic spectrophotometer (Perkin Elmer 2280). Dissolved oxygen was measured by iodometric (Winkler) method (APHA 1998); oxidizable compounds by manganometric method (APHA 1998); nitrate by ultraviolet spectrophotometry (APHA 1998), nitrite and ammonia by colorimetric determination, with Pharmacia LKB Ultraspec Plus (APHA 1998; Estrada 1986). Phosphate measurement was by ascorbic acid method (APHA 1998; Rodier 1998).

For metal analysis, the residue dried was redissolved in acid mixture (2 mL HCl 50% vol/vol + 2 mL HNO<sub>3</sub> 50% vol/vol), with filtered and double-distilled water added to complete 25 mL (Tenorio Sanz 1988). After this preparation Cu, Fe, Mn, Zn, Pb, Ni, Co, Cd, and Cr were determined by FAAS with a Perkin-Elmer 2280 system, using oxidizing air-acetylene flame (except for Cr). Instrument operating conditions are presented in Table 1. Calibration solutions were purchased from Panreac Química S.A.

The analytical procedure was tested for both measurement precision and accuracy in order to assess the degree of reliability which can be allocated to the data generated by this investigation. The precision of the method was established by a calculation of between-assay variation coefficients from data from five analysis carried out at different times on a water sample. The coefficients of variation obtained in all

**Table 1.** Perkin-Elmer 2280 conditions for the determination of heavy metals

Element	$\lambda$ /slit	Accuracy (% recovery)	Precision (%)	Sensitivity (mg/L)
Cu	324.8 nm/0.7	102.0	4.97	0.032
Fe	248.4 nm/0.2 271.9 nm/0.2	104.0	8.24	0.039 0.12
Mn	279.5 nm/0.2	98.2	7.33	0.03
Zn	213.9 nm/0.7	101.2	1.49	0.015
Pb	217.0 nm/0.7	102.6	5.53	0.079
Ni	232.0 nm/0.2	100.8	2.45	0.042
Cr	357.9 nm/0.7	98.0	8.82	0.041
Co	240.7 nm/0.2	102.4	2.30	0.075
Cd	228.8 nm/0.7	101.0	2.72	0.016

cases were reasonable (Table 1). The level of accuracy was monitored by recovery test. The recovery percentages were near 100% (Table 1).

### Data Analysis

A rough estimate of physical and chemical processes present in analyzed waters was developed by Component Analysis, performed with SPSS version 10 statistical package. This analysis allows us to ascertain the origin of each element based on its level of association with the others and to determine the factors that control its hydrochemical behavior. The method reduces the original variables to a smaller number of factors, those represent the original variables with a minimal loss of information. Hardness and bicarbonate content were excluded in this analysis: the first because of its close dependence with calcium and magnesium content; the second because it was only present in OD-A. Seven factors were extracted from the first matrix, accounting for 93.20% total variance. In order to improve this solution, we applied a rotation by VARIMAX standardization (that maximizes the sum of variance loadings in the factor matrix) to obtain the rotated component matrix that is shown in Table 2. VARIMAX rotation allows better distribution of factorial loadings, mainly in the last factors. Other rotations, both orthogonal and oblique, did not improve this solution.

### Results and Discussion

Odiel water samples were characterized by low pH values downstream the Iberian Pyrite Belt. pH values were within the range of 2.76 to 3.71, according to the values typically found in acid drainage waters (López Pamo 1999; Monterroso 1998). This high acidity causes large quantities of the constituent elements to be made soluble. Consequently, we observed high dissolved solid content (1484–10003.5 mg/L) and electric conductivity levels (1410.08–6118.33  $\mu$ S/cm).

This degree of salinization was due to the massive sulfate presence in analyzed waters (1579–4004 mg  $\text{SO}_4^{2-}$ /L, Table 6), as a result of the sulfide oxidation in these naturally mineralized areas (IGME 1982) and mining residues. Sulfate variation in the studied zone showed a behavior similar to that of dissolved solids and conductivity (Table 4), which is the general pattern: a high increase from OD-A and OD-B (where the Odiel River crosses the Spanish Pyrite Belt and manganese ores), a drop from OD-B to OD-C, due to the dilution of these

discharges along the river stream, and a new increase in OD-D, because of new discharges near the Sotiel-Coronada mine. Hardness showed a similar pattern: we find high values (1210–5200 mg  $\text{CaCO}_3$ /L, Table 4), due to the high content of calcium (Ca) (48–568 mg/L) and, above all, of magnesium (Mg) (190.75–915.07 mg Mg/L, Table 5).  $\text{MgSO}_4$  attached to metal sulfate ores dissolves more easily than  $\text{CaSO}_4$  (Catalán Lafuente and Catalán Alonso 1987). However, in OD-D the relation between the two sulfates was inverted because of differences in lithology (IGME 1982).

Other cations and anions were less significant (Tables 3 and 5). Chloride content was low and relatively steady (24.62–79 mg  $\text{Cl}^-$ /L, Table 6) because its content was unaffected by mine drainage. There was no substantial variation along the length of the river and OD-A showed a similar—and even higher—content than the other sampling zones. OD-A levels could come from weathering of catchment bedrock (Sullivan and Drever 2001) and the pollution source supplied by nearby cattle. Bicarbonates were only present in OD-A because of its pH value. Silicon (Si) content was low along the river stream (7.63–21.05 mg/L), but higher in LOM (33.25–45.40 mg/L).

Sodium (Na) content (Table 5) remained relatively constant along the Odiel River. It reached higher values in OD-A zone (23.23–51.50 mg/L), but values in LOM were even higher (117–191.13 mg/L). Potassium (K) content was lower than Na content, as generally occurs in natural waters (Catalán Lafuente and Catalán Alonso 1987).

Dissolved oxygen content in OD-A was very high, almost reaching saturation values. A heavy degradation occurs along the length of the river stream, so there is practically no dissolved oxygen in OD-D (Table 3). For this reason, the highest values of COD were measured at this point.

Nitrogen (N) components (Table 3) showed low values along the river, but nitrate content rose slightly in OD-B. Ammonia was at a maximum in LOM (0.73 mg  $\text{NH}_4^+$ /L) and we hypothesized that it came from nearby cattle urine. In OD-A, we measured the highest concentrations of nitrite, nitrate, ammonia, and phosphate, so their common source could be fertilizer application.

The majority metals were iron (Fe), zinc (Zn), manganese (Mn), and copper (Cu). All of these showed the general pattern. Cu concentrations in LOM were lower due to the different composition of the mineral ores of this zone (Pérez Macías 1996). Of the minority metals, nickel (Ni), cobalt (Co), and cadmium (Cd) showed a pattern that was characterized by reaching a maximum in OD-B, and by the dilution of these concentrations along the river. LOM showed lower contents. Lead (Pb) reached its maximum in OD-D and LOM, and chromium (Cr) was low, even absent, at all the studied points.

### Multivariate Analysis: First Component

According to our analysis, the first component included: conductivity, total dissolved solids, sulfate, Ca, Mg, Na, Si, ammonia, and Fe. Almost all of these variables were related with: the products of pyrite oxidation; the salts that are solubilized by the high acidity generated in the oxidation of sulfides. It accounted for 40.88% of total variance.

**Table 2.** Rotated component matrix by component analysis, VARIMAX applied (significant loadings in **bold**)

	Components						
	1	2	3	4	5	6	7
Water temp	.111	3.674E-02	.176	-.148	<b>.929</b>	.129	-.177
pH	-.401	-.599	-.544	.225	.265	3.825E-02	-4.647E-02
Conductivity	<b>.851</b>	.138	.364	-.136	.163	-1.401E-02	9.645E-02
TDS	<b>.946</b>	.216	8.542E-02	-.111	6.548E-02	-1.508E-02	7.608E-02
Ca	<b>.877</b>	.145	.222	1.585E-02	-.106	.120	.214
Mg	<b>.896</b>	.182	.165	-.140	-.150	.129	.225
Na	<b>.906</b>	-.371	7.215E-02	-2.272E-03	8.815E-02	-4.150E-02	-5.724E-02
K	-.306	-.598	9.786E-02	.309	.497	-.172	-.149
Cl	5.120E-02	-.457	8.414E-02	6.085E-02	2.435E-02	<b>.827</b>	.136
Sulfate	<b>.932</b>	.226	.233	-.130	-1.213E-02	-2.525E-02	5.899E-02
Silica	<b>.911</b>	1.944E-02	.105	-.234	.146	.146	-4.892E-02
COD	.390	-.365	.451	1.227E-02	-.286	-.488	.288
Dissolved O <sub>2</sub>	-.196	-9.293E-02	<b>-.913</b>	.192	-4.860E-02	-.132	-5.063E-03
Nitrate	.289	6.075E-02	-9.194E-02	2.234E-03	-.130	3.232E-02	<b>.920</b>
Nitrite	-.222	-.196	-.387	.763	-5.363E-02	.174	.214
Ammonia	<b>.888</b>	-.421	-4.141E-02	7.681E-02	-3.995E-03	-7.350E-02	8.796E-02
Phosphate	-.335	-.566	-.583	.420	7.602E-02	-9.665E-02	-7.879E-02
Cu	-7.810E-02	<b>.821</b>	-.316	5.229E-02	-.157	-9.393E-02	-6.211E-03
Fe	<b>.826</b>	8.981E-02	.151	9.525E-02	-.190	-.271	-.142
Mn	-5.996E-02	.150	-.123	<b>.895</b>	-1.546E-02	-8.574E-02	-.106
Zn	.571	.758	4.598E-04	.191	-.109	-.122	-.125
Pb	.368	-3.035E-02	<b>.725</b>	-.134	.246	-7.304E-02	-.209
Ni	6.946E-02	<b>.964</b>	.199	-5.528E-04	6.041E-02	-6.000E-02	5.737E-03
Cr	8.662E-02	.286	.153	-.169	-.664	.596	-.139
Co	-4.510E-02	<b>.973</b>	.157	-1.530E-02	-1.366E-02	-6.505E-02	7.118E-03
Cd	8.086E-02	<b>.978</b>	9.800E-02	-1.525E-02	6.177E-02	2.582E-02	9.008E-02

**Table 3.** Contamination parameters in analyzed water samples

Zone	COD <sup>a</sup> (mg O <sub>2</sub> /L)	Dissolved oxygen (mg O <sub>2</sub> /L)	Nitrate (mg NO <sub>3</sub> <sup>-</sup> /L)	Nitrite (mg NO <sub>2</sub> <sup>-</sup> /L)	Ammonia (mg NH <sub>4</sub> <sup>+</sup> /L)	Phosphate (mg PO <sub>4</sub> <sup>3-</sup> /L)
<b>July 1998</b>						
OD-A	5.76 ± 0.39	8.37	1.56	0.1	0.09	0.26
OD-B	4.02 ± 0.43	5.58	10.70	0.05	0.03	0
OD-C	3.59 ± 0.39	2.58	1.05	0.05	0	0
OD-D	14.14 ± 1.27	0	1.00	0	0.02	0
LOM	11.82 ± 0.04	1.44	0	0.05	0.70	0
<b>March 1999</b>						
OD-A	6.33 ± 0.15	6.03	4.51	0.24	0.24	0.32
OD-B	4.04 ± 0.42	2.83	19.27	0.22	0.05	0
OD-C	3.25 ± 0.23	4.36	5.42	0	0	0.03
OD-D	5.46 ± 1.34	0.99	9.57	0	0.03	0
LOM	6.57 ± 0.33	1.94	7.19	0	0.43	0.02
<b>November 1999</b>						
OD-A	6.70 ± 0	12.24	5.13	0.21	0.14	0.33
OD-B	7.59 ± 0.40	6.39	8.20	0.06	0.10	0.04
OD-C	3.72 ± 0.17	5.92	2.15	0.06	0.03	0.03
OD-D	18.58 ± 0	0.12	2.33	0.08	0.03	0.02
LOM	21.25 ± 0.16	4.27	27.88	0.05	0.73	0.04

<sup>a</sup> mean ± SD, n = 3.

*Electric Conductivity and Dried Residue.* Both variables showed similar behavior in the Odiel River, as well as in LOM (Table 4). Salts are dissociated because of extremely acidic pH. We can thus define a linear relationship between both parameters with a high correlation coefficient:  $r = 0.9770$ ;  $p < 0.001$ .

*Sulfate, Calcium, Magnesium, and Iron.* Most of the properties of this water depended on sulfate concentration as it was present in large amounts. Linear correlations between sulfate and the rest of the 26 analyzed parameters were developed and the highest correlations were the following ( $p < 0.001$ ): total

**Table 4.** General physicochemical parameters in analyzed water samples

Zone	Water temp. (°C)	pH	Turbidity (UNF)	Conductivity (µS/cm)	TDS <sup>a</sup> (mg/L)	Hardness <sup>a</sup> (mg CaCO <sub>3</sub> /L)
<b>July 1998</b>						
OD-A	26	8.39	4	486.91	305.13 ± 7.68	250 ± 6
OD-B	26	2.87	9	3648.14	5602.16 ± 70.96	2210 ± 50
OD-C	29	2.89	<1	2619.63	3235.17 ± 33.52	1230 ± 70
OD-D	24	2.83	<1	2971.26	3173.67 ± 23.17	1800 ± 40
LOM	25	2.76	<1	6118.33	10003.50 ± 4.26	5200 ± 100
<b>March 1999</b>						
OD-A	18	6.50	6	427.47	288.60 ± 4.33	180 ± 0
OD-B	18	3.45	12	2474.47	3540.67 ± 32.41	2900 ± 0
OD-C	16	3.51	5	1410.08	1484.00 ± 65.00	1350 ± 50
OD-D	19	3.39	<1	1983.21	2106.50 ± 34.71	1210 ± 10
LOM	24	3.33	<1	4552.53	6827.17 ± 19.64	4090 ± 10
<b>November 1999</b>						
OD-A	10	6.50	<1	469.84	289.33 ± 2.45	224 ± 0
OD-B	10	2.92	16	2888.62	5290.83 ± 16.58	3100 ± 50
OD-C	9	2.91	2	2566.70	4016.17 ± 19.83	2160 ± 60
OD-D	10	2.81	<1	2505.79	3335.17 ± 34.56	1890 ± 30
LOM	12	2.96	3	4663.02	8735.00 ± 29.77	5150 ± 50

<sup>a</sup> Results expressed as mean ± SD, *n* = 3.

**Table 5.** Main cations in analyzed water samples

Zone	Ca (mg/L)	Mg (mg/L)	Na (mg/L)	K (mg/L)
<b>July 1998</b>				
OD-A	52.00 ± 0.35	287.86 ± 0.79	27.90 ± 1.55	10.95 ± 0.60
OD-B	150.10 ± 31.02	490.60 ± 68.76	30.67 ± 5.97	2.69 ± 0.80
OD-C	126.25 ± 0.83	231.88 ± 3.22	31.1 ± 0.35	2.40 ± 0.02
OD-D	353.13 ± 6.84	190.75 ± 25.26	48.61 ± 4.82	7.43 ± 1.43
LOM	556.00 ± 12.00	915.07 ± 16.82	191.13 ± 1.20	4.40 ± 0.68
<b>March 1999</b>				
OD-A	47.20 ± 5.60	12.04 ± 0	51.05 ± 3.35	9.81 ± 0.88
OD-B	380.00 ± 3.00	561.70 ± 86.50	22.45 ± 1.25	2.28 ± 0.18
OD-C	48.00 ± 24.00	295.20 ± 26.40	25.51 ± 6.11	3.15 ± 0.14
OD-D	84.00 ± 4.00	237.60 ± 2.40	25.02 ± 6.20	3.54 ± 0.72
LOM	504.00 ± 0	679.20 ± 0	117.00 ± 3.00	1.70 ± 0.09
<b>November 1999</b>				
OD-A	46.40 ± 0	25.97 ± 0	42.63 ± 2.59	2.53 ± 0.06
OD-B	483.50 ± 24.50	453.70 ± 26.50	25.91 ± 3.05	1.66 ± 0.17
OD-C	177.20 ± 0	412.08 ± 10.21	23.37 ± 3.01	1.54 ± 0.30
OD-D	196.00 ± 2.50	336.00 ± 8.50	23.23 ± 2.76	3.11 ± 0.28
LOM	568.00 ± 8.00	895.2 ± 16.10	141.06 ± 23.87	2.66 ± 0.49

Results expressed as mean ± SD, *n* = 3.

dissolved solids,  $r = 0.9969$ ; conductivity,  $r = 0.9895$ ; hardness,  $r = 0.9577$ . Sulfate predominance was the main cause of high levels of dried residue and conductivity. The high acidity generated during the oxidizing process is able to accelerate the solubilization of other minerals, such as Ca and Mg. Because Ca and Mg play a part in hardness, there is a high sulfate–hardness correlation ( $p < 0.001$ ):  $\text{SO}_4^{2-}$ –Mg,  $r = 0.9501$ ;  $\text{SO}_4^{2-}$ –Ca,  $r = 0.8996$ . There was also a sharp increase in iron concentration in OD-B, which is lightly diluted between OD-C and OD-D (Figure 2). Fe content in LOM zone reflects the high amount of this metal in nearby ores.

*Sodium, Silica, and Ammonia.* The importance of these variables was slight. They appear in this component because they

all rose dramatically in OD-B and LOM, as did the main salts studied. The highest sodium–anion correlation was Na–Si ( $r = 0.8331$ ,  $p < 0.001$ ). Ammonia presence in this component was due to its correlation with sodium, and we hypothesized that cattle urine was the source of these elements.

#### *Multivariate Analysis: Second Component*

The second component included Ni, Co, Cd, Cu, Zn, pH, and K. It accounted for 21.05% of total variance (accumulated 61.93%). These heavy metals and pH are linked to the discharge in OD-B. Cu and Zn showed lower factorial loadings up



**Table 6.** Anions in analyzed water samples

Zone	Chloride (mg Cl <sup>-</sup> /L)	Bicarbonate (mg H <sup>-</sup> CO <sub>3</sub> /L)	Silicate (mg/L)	Sulfate (mg SO <sub>4</sub> <sup>2-</sup> /L)
<b>July 1998</b>				
OD-A	58.45 ± 0	212.52 ± 2.34	10.60 ± 0.65	47.48 ± 1.23
OD-B	29.22 ± 0	–	21.05 ± 0.80	4004.93 ± 21.40
OD-C	24.62 ± 0.91	–	20.40 ± 0.05	2286.56 ± 6.59
OD-D	45.60 ± 1.83	–	14.05 ± 0.15	2442.10 ± 175.30
LOM	51.07 ± 1.82	–	42.25 ± 0.65	6940.48 ± 32.10
<b>March 1999</b>				
OD-A	50.28 ± 0	170.00 ± 2.10	4.42 ± 0.04	69.71 ± 7.82
OD-B	79.00 ± 7.18	–	11.95 ± 0.05	2462.50 ± 3.50
OD-C	46.68 ± 3.59	–	7.63 ± 0.03	1086.00 ± 13.00
OD-D	46.68 ± 3.59	–	8.08 ± 0.03	1579.00 ± 41.00
LOM	79.00 ± 7.18	–	45.40 ± 0.02	4830.50 ± 135.50
<b>November 1999</b>				
OD-A	51.22 ± 0.50	176.78 ± 2.20	5.65 ± 0.04	119.33 ± 0.83
OD-B	31.79 ± 0.34	–	16.95 ± 0.20	3335.50 ± 35.50
OD-C	38.85 ± 2.55	–	15.65 ± 0.30	2695.00 ± 51.00
OD-D	47.68 ± 1.23	–	12.00 ± 0.05	2207.00 ± 29.00
LOM	37.09 ± 1.44	–	33.25 ± 0.50	5730.00 ± 192.00

Results expressed as mean ± SD, *n* = 3.

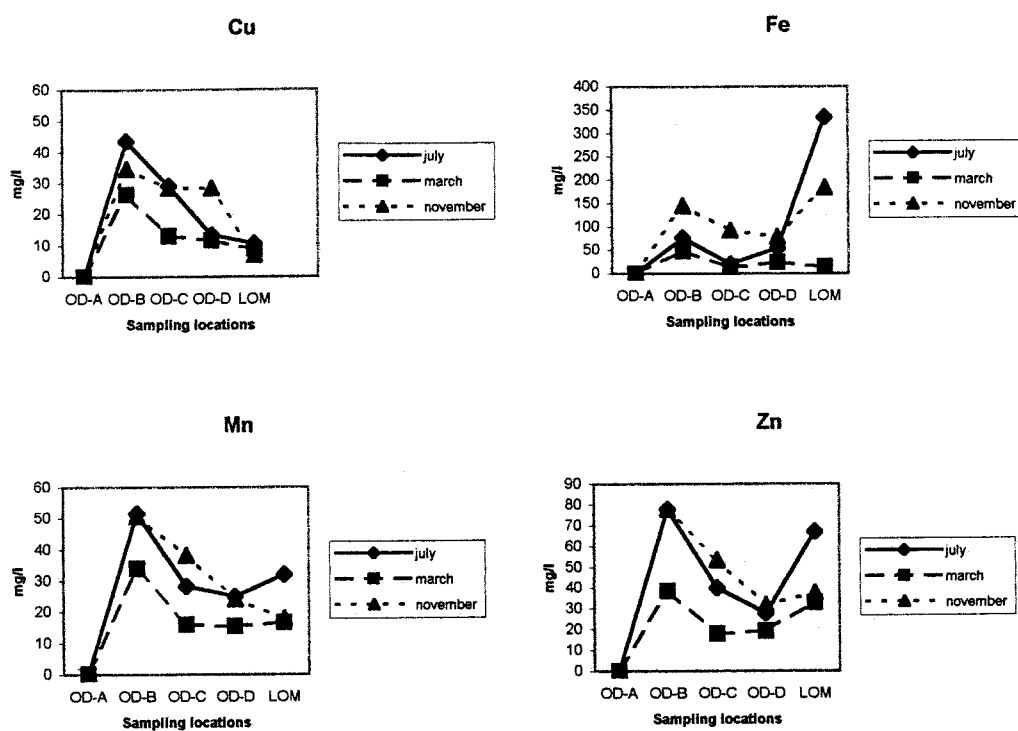


**Fig. 2.** Metal content in water for Cu, Fe, Mn, and Zn in the Odiel River and El Lomero Mines for the different seasons and sampling zones

this component; K content (which showed negative factorial loading) is of less importance. This heavy metal group is consistent with the observations from other studies (Grande *et al.* 1999; Naicker *et al.* 2003), which highlight the fact that all of these are metals which have a single stable oxidation state.

**Nickel, Cobalt, and Cadmium.** These three metals are linked to this factor due to their similar behavior, which is characterized

by a sharp increase in OD-B and decreasing concentrations along the river (Figure 3); discharges of these metals in OD-D must therefore be slight. This similar behavior is also revealed by the correlation coefficients ( $p < 0.001$ ): Ni–Co,  $r = 0.9867$ ; Ni–Cd,  $r = 0.9838$ ; Co–Cd,  $r = 0.9837$ .

**Copper and Zinc.** There was a sharp increase in Cu and Zn concentration from OD-A to OD-B zones (Figure 2). However,

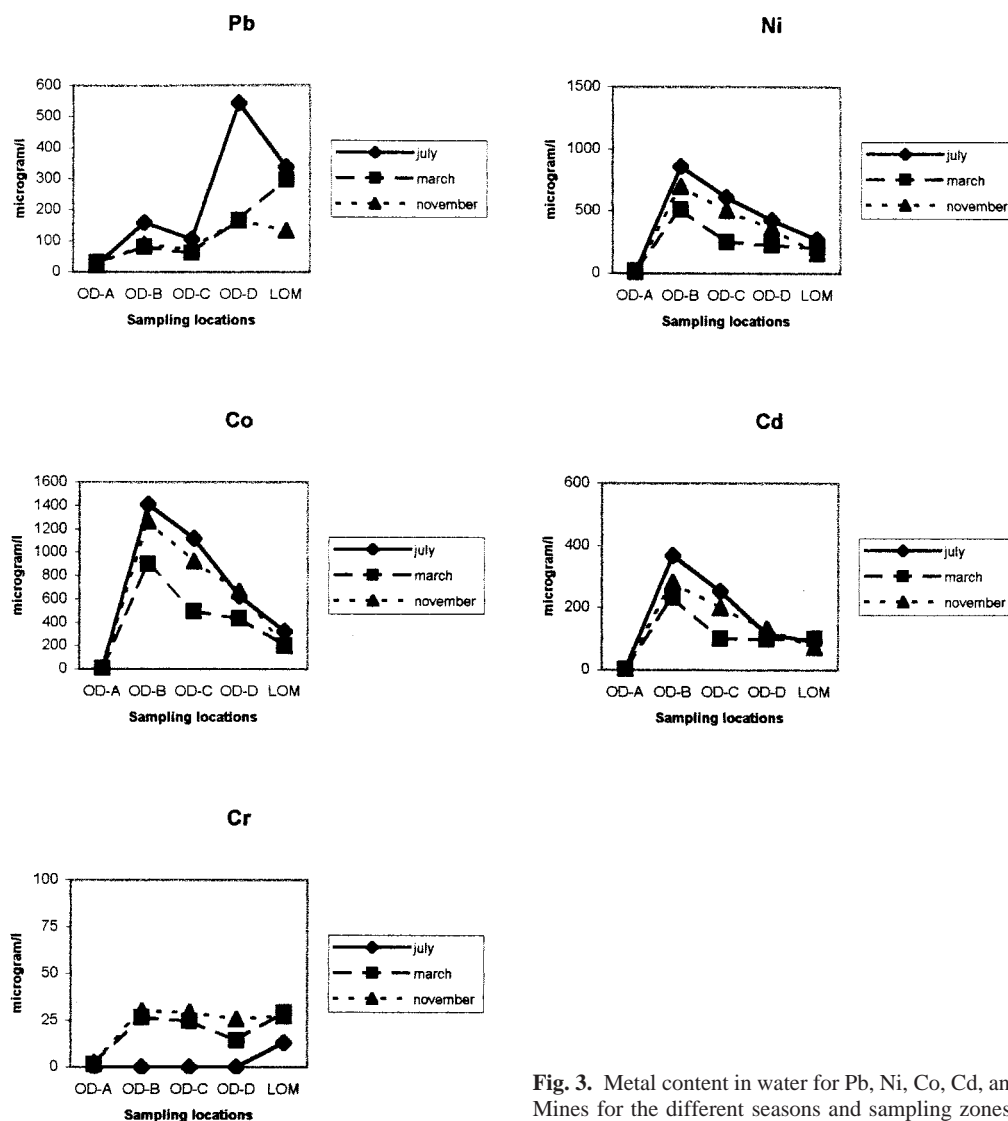


Fig. 3. Metal content in water for Pb, Ni, Co, Cd, and Cr in the Odiel River and Lomero Mines for the different seasons and sampling zones

this level remained virtually constant for Cu, summer sampling excluded. In general, Zn levels diminished along the length of the river (Figure 2). OD-D ores have a lower Zn content than those of San Platón, near OD-B zone (Pérez Macías 1996).

**pH.** When the Odiel River begins to cross mineral ores in the Iberian Pirite Belt (El Soldado, La Poderosa, Concepción y San Platón), it receives acid discharges that lowered pH to values around 3, remaining almost constant along the river (Table 4). In OD-D, pH value reflected fresh contributions, and consequently this point showed the lowest river pH. LOM pH showed a similar behavior. K is related to this component because of its correlation with pH, which we believe to be coincidental.

#### Multivariate Analysis: Third Component

The third component was related with the variables specifically affected by the discharge in OD-D. It accounted for 10.45% of

total variance (accumulated 72.4%) and is positively related with the Pb content (which increased in OD-D) and negatively related with dissolved oxygen (which dropped in OD-D). Increases in Pb levels (Figure 3), probably due to mining discharges, appeared more clearly in summer because of a decrease in the river flow.

#### Multivariate Analysis: Fourth Component

The fourth component included Mn and nitrites. It accounted for 7.66% of total variance (accumulated 80.04%). Mn behavior was similar to that of Fe (Figure 2). Correlation coefficient between these is usually high in natural environments (water, soil), but not in this case ( $r = 0.2705$ , OD-A excluded due to its much lower values). The observed increase in OD-B was due to the Odiel passing through Mn ores, about 4 km upstream. LOM showed similar contents to the Odiel River. We

believe correlation between Mn and nitrites ( $r = 0.5942$ ,  $p = 0.015$ ) to be coincidental.

### Multivariate Analysis: Fifth Component

The fifth component accounted for 5.24% of total variance (accumulated 85.28%). Water temperature and Cr content were respectively directly and inversely related to this component. Cr relation with water temperature in this component was due to the seasonality of both variables. In summer, water temperature increases. In addition, chromium precipitates as a consequence decrease in the flow.

The last components included chloride and nitrate. There is no relationship because both variables reach their maximum in spring, and they have different sources unrelated with sulfur and manganese ores. The correlation coefficient between chloride and electric conductivity was  $r = -0.033$ ,  $p = 0.91$ ; so chloride influence in water salts was low.

### Seasonal Variation

Sulfate content and its related variables (dissolved solids and electric conductivity) were higher for samples taken in July because of lower water flow. The lowest pH values were reached in July and November. Na content was higher in July because of the drop in water flow, especially in LOM. Chloride content showed little seasonal variation. Because of temperature speeds up Si dissolution (Catalán Lafuente and Catalán Alonso 1987), the highest values occurred in July (Table 6).

### Heavy Metals

In our study of heavy metals in the Odiel River and El Lomero mines, we observed three different seasonal patterns. The first appeared in majority metals, whose concentrations in water were of the order of mg/L: Cu, Fe, Mn, Zn. These metals showed concentrations which follow the order November > July > March (Figure 2). Low Cu content in LOM, without seasonal variation, was due to the different composition of its ores: San Platón pyrite (near OD-B zone) shows 6.50% Cu; LOM pyrite shows a high Fe content, while Cu content in this zone is around 1.50–1.90% (Pérez Macías 1996).

The second pattern appeared in minority metals, whose concentrations in water were of the order of  $\mu\text{g/L}$ : Pb, Ni, Co, Cd. These metals showed concentrations which follow the order July > November > March (Figure 3). The third pattern appeared in Cr: November > March > July.

It has been reported that the behavior of Fe, Cu, and Zn in acidic waters is strongly controlled by precipitation (Dinelli *et al.* 2001). In our case, this different behavior was due to salt efflorescence as the majority metal deposit (Gray 1998; López-Pamo *et al.* 1999). In summer, evaporation of acidic waters produced a layer of efflorescent salts mainly made up of hydrated metal sulfates (Keith *et al.* 2001) and the dissolved metal content therefore dropped. Early rainfall in autumn dissolved efflorescence and the salts returned to the river bed, so metal content increased.

The concentration of minority metals is apparently not high enough to precipitate, or the amount of precipitation amount may be insignificant. Higher concentration is therefore reached in summer due to water flow decrease. Flow effect also explained lower metal levels in the spring sampling, as there were no salt coatings to provide fresh salts.

Cr behavior could be explained due to its importance in vauquelinite efflorescence,  $\text{Pb}_2\text{Cu}(\text{CrO}_4)(\text{PO}_4)(\text{OH})$ , (MA Vicente, personal communication) together with the great insolubility of chromium salts formed (for instance,  $\text{PbCrO}_4$  has a  $K_s = 1.8 \cdot 10^{-14}$ ). Cr is the least movable of heavy metals (Catalán Lafuente and Catalán Alonso 1987) and it is able to quickly form hydroxides, oxides, and complexes (Babich and Stotzky 1983). Thus, Cr disappeared from the stream in summer (Figure 3).

Pb balance, which is also a component of vauquelinite, may depend on lead sulfate, whose solubility ( $K_s = 1.6 \cdot 10^{-8}$ ) is between that of barium sulfate ( $K_s = 1.3 \cdot 10^{-10}$ ) and calcium sulfate ( $K_s = 1.2 \cdot 10^{-6}$ ). Pb therefore remained in solution during summer, when it reached its highest concentrations.

### Conclusions

The characteristics of the Odiel River's water are mainly related to its sulfate content. Sulfate comes from sulfide oxidation, and in this study, reached its maximum level in summer due to the drop in the water flow. The high acidity thus generated caused salt solubilization and an increase in metals. The amounts of heavy metals in the river are related to the role played by efflorescences. These acted as a metal reserve in summer and as a source in autumn, when they dissolved again. Three groups of heavy metals were distinguished according to their quantities in the stream and their solubility. In order of importance they were: majority metals (Cu, Fe, Mn, Zn); minority metals (Pb, Ni, Co, Co); and Cr.

### References

- APHA (1998) Standard methods for the examination of water and wastewater. Washington, DC.
- Belén M (2000) El país: Territorio y poblamiento. Argantonio, rey de Tartessos, Fundación el Monte, Sevilla, pp 79–117
- Blasco Gordo V (1983) Métodos de análisis químicos de aguas. MICOV, Valencia
- Caruccio F, Hossner L, Geidel G (1989) Pyritic materials: Acid drainage, soil acidity, and liming. In: Hossner LR (ed) Reclamation of surface-mined lands. CRC Press, Boca Raton, Florida, pp 129–148
- Catalán Lafuente J, Catalán Alonso JM (1987) Ríos, caracterización y calidad de sus aguas. Ed Dihidrox, Madrid
- Dinelli E, Lucchini F, Fabbri M, Cortecchi G (2001) Metal distribution and environmental problems related to sulfide oxidation in the Libiola copper mine area. J Geochem Explor 74:141–152
- Elbaz-Poulchet F, Morley NH, Cruzado A, Velasquez Z, Achterberg EP, Braungardt CB (1999) Trace metal and nutrient distribution in an extremely low pH (2.5) river–estuarine system, the Ria of Huelva (south-west Spain). Sci Total Environ 227:73–83
- Estrada P (1986) Manual de control analítico de la potabilidad de las aguas de consumo humano. Ed. Díaz de Santos, Madrid
- Evangelou V, Zhang Y (1995) A review: Pyrite oxidation mechanism



- and acid mine drainage prevention. *Crit Rev Environ Sci Technol* 25:141–199
- García Vargas M, Ruiz-Abrio MT, Guerrero MA (1980) Determinación de metales pesados por espectroscopía de absorción atómica en la cuenca del río Tinto. *Técnicas en Investigación del Medio Ambiente* 2:12–24
- Grande J, Borrego J, Morales J (1999) A study of heavy metal pollution in the Tinto–Odiel estuary in southwestern Spain using factor analysis. *Environ Geol* 39:1095–1101
- Gray N (1997) Environmental impact and remediation of acid mine drainage: A management problem. *Environ Geol* 30:62–71
- Gray NF (1998) Acid mine drainage composition and the implications for its impact on lotic systems. *Water Res* 32:2122–2134
- IGME (1982) Mapa geológico de España. Ministerio de Industria y Energía, Madrid, p 938
- Keith DC, Runnells DD, Esposito KJ, Chermak JA, Levy DB, Hannula SR, *et al.* (2001) Geochemical models of the impact of acidic groundwater and evaporative sulfate salts on Boulder Creek at Iron Mountain, California. *Appl Geochem* 16:947–961
- López-Pamo E, Baretino D, Antón-Pacheco C, Ortiz G, Arránz JC, Gumiel JC, *et al.* (1999) The extent of the Aznalcóllar pyritic sludge spill and its effects on soils. *Sci Total Environ* 242:57–88
- Lowson RT (1982) Aqueous oxidation of pyrite by molecular oxygen. *Chem Rev* 82:461–497
- Naicker K, Cukrowska E, McCarthy TS (2003) Acid mine drainage arising from gold mining activity in Johannesburg, South Africa and environs. *Environ Pollut* 122:29–40
- Nelson CH, Lamothe PJ (1993) Heavy metal anomalies in the Tinto and Odiel river and estuary system, Spain. *Estuaries* 16:495–511
- Pérez Macías JA (1996) La producción de metales en el cinturón ibérico de piratas en la prehistoria y antigüedad. Tesis Doctoral. Universidad de Huelva
- Quesada C (1996) Estructura del sector español de la faja piritica. Implicaciones para la exploración de yacimientos. *Boletín Geológico y Minero* 107:265–278
- Rambaud Pérez F (1963) Notas geológico-estructurales de la zona norte de Riotinto (Huelva). *Estudios Geológicos* 19:67–69
- Rodier J (1998) Análisis de las aguas. Aguas naturales, aguas residuales, agua de mar, Ed. Omega, Barcelona
- Sullivan AB, Drever JI (2001) Spatiotemporal variability in stream chemistry in a high-elevation catchment affected by mine drainage. *J Hydrol* 252:237–250
- Tenorio Sanz MD (1988). Estudio de metales pesados y otros parámetros indicativos de la calidad de las aguas del río Jarama. Tesis Doctoral. Universidad Complutense, Madrid.
- van Geen A, Adkins JF, Boyle EA, Nelson CH, Palanques A (1997) A 120 year record of widespread contamination of the Iberian pyrite belt. *Geology* 25:291–294
- van Geen A, Takesue R, Chase Z (1999) Acid mine tailings in southern Spain. *Sci Total Environ* 242:221–229